Technical University of Denmark

DTU

Topology Optimization for Conceptual Design of Reinforced Concrete Structures

Amir, Oded; Bogomolny, Michael

Link back to DTU Orbit

DTU Library
Technical Information Center of Denmark

Topology Optimization for Conceptual Design of Reinforced Concrete Structures

Oded Amir[1] **and Michael Bogomolny**[2]

[1]Dept. of Mechanical Engineering, Technical University of Denmark, Lyngby, Denmark, odam@mek.dtu.dk
[2]Plasan, Research and Development Department, Sasa, Israel, michaelbo@plasan.com

1. Abstract
Design of reinforced concrete structures is governed by the nonlinear behavior of concrete and by its different strengths in tension and compression. The purpose of this article is to present a computational procedure for optimal conceptual design of reinforced concrete structures, based on topology optimization with elasto-plastic material modeling. Concrete and steel are both considered as elasto-plastic materials, including the appropriate yield criteria and post-yielding response. The same approach can be applied also for topology optimization of other material compositions where nonlinear response must be considered. Optimized distribution of material is achieved by introducing interpolation rules for both elastic and plastic material properties. Several numerical examples illustrate the capability and potential of the proposed procedure.

2. Keywords: Topology design, Plasticity, Reinforced concrete.

3. Introduction
Structural optimization techniques are now becoming an integral part of the design process and are widely applied, for example, in the automotive and aerospace industries. So far, optimal design had less impact on traditional structural engineering as practiced in the construction industry. One reason might be the difficulty in combining numerical optimization tools with models that can accurately represent the complex behavior of composite materials used by the building industry, such as reinforced concrete. The aim of this article is to present a computational procedure that enables optimal design of reinforced concrete structures. The approach can easily be generalized to accommodate other combinations of materials besides steel and concrete. By combining topology optimization with elasto-plastic modeling of the candidate materials, it is possible to consider not only the different elastic stiffnesses of the candidate materials, but also their distinct yield limits and yield criteria.

Up to date, the vast majority of studies in structural topology optimization were restricted to elastic material models (see Bendsøe and Sigmund [3] for a comprehensive review of the field). Elastic modeling is sufficient for determining the distribution of one or more material phases in a given domain, but only as long as all material points remain in their elastic stress state. This is clearly not the case in reinforced concrete, where the concrete phase fails under relatively low tension stresses. Therefore nonlinear material modeling is necessary when aiming at optimal design of RC structures. Several studies were dedicated to topology optimization of elasto-plastic structures, for example based on the von Mises yield criterion [21, 15] or the Drucker-Prager yield criterion [21]. However, to the best of the authors' knowledge, this is the first study where more than one nonlinear candidate material is considered. Lately, multiphase material optimization was utilized for improving the performance of fiber reinforced concrete [10]. Failure behavior of all candidate materials was considered, but the approach taken is restricted to layered structures and cannot provide general layouts as obtained using topology optimization.

One approach to visualizing the internal forces in cracked concrete beams is by a simple truss model introduced by Ritter [17]. The resulting model, widely known as the strut-and-tie model, has numerous applications in analysis and design of RC structures subjected to shear forces or torsion moments (e.g. Schlaich et al. [18], Marti [14]). Several researchers proposed to use a truss-like structure resulting from linear elastic topology optimization in order to predict a strut-and-tie model (Bruggi [5], Liang et al. [12] and Kwak and Noh [11]). Accordingly, the truss bars under tension forces represent the location of steel reinforcement while the compressed bars represent concrete. In the current study material nonlinearity of both concrete and steel is considered , and hence a more realistic model is obtained. An interpolation scheme is proposed, such that by changing the density (design variable of the optimization problem), the material properties and the failure criteria vary between concrete and steel. The result of the optimization

process is the optimal distribution of concrete and steel inside a certain domain. Therefore an efficient strut-and-tie model is directly obtained.

5. Nonlinear material model and finite element analysis

In this section, we shortly review the elasto-plastic model utilized in our study and outline the resulting nonlinear finite element problem to be solved. Later, in Section 6, the connection between the topology optimization problem and the nonlinear material model will be made.

The main purpose of this study is to optimize the distribution of two materials in a given domain, taking the different nonlinear behavior of both materials into account. The main idea is to represent the elasto-plastic response of both materials using one generic yield function that varies according to the value of the design variable. For this purpose, we utilize the Drucker-Prager yield criterion [9]. For certain choices of material properties, the Drucker-Prager yield function can model the behavior of materials that are much stronger in compression than in tension, such as soils, rock or plain concrete. Moreover, the von Mises yield criterion which is widely used for metals (having equal strength in tension and compression) can be seen as a particular case of the Drucker-Prager criterion.

In the following, we present the governing equations of the elasto-plastic model, leading to the local constitutive problem to be solved on a Gauss-point level. We follow classical rate-independent plasticity formulations, based on the textbooks by Simo and Hughes [19] and Zienkiewicz and Taylor [22]. The Drucker-Prager yield function can be expressed as

$$f(\boldsymbol{\sigma}, \kappa) = \sqrt{3J_2} + \alpha(\kappa)I_1 - \sigma_y(\kappa) \leq 0$$

where J_2 is the second invariant of the deviatoric stress tensor and I_1 is the first invariant (trace) of the stress tensor. α is a material property and σ_y is the yield stress in uniaxial tension, both functions of the internal hardening parameter κ according to some hardening functions. The expression $\sqrt{3J_2}$ is usually known as the *von Mises stress* or *equivalent stress*. When $\alpha = 0$, we obtain the von Mises yield criterion. We assume simple isotropic hardening rules

$$\begin{aligned} \alpha(\kappa) &= constant & (1) \\ \sigma_y(\kappa) &= \sigma_y^0 + HE\kappa & (2) \end{aligned}$$

where σ_y^0 is the initial uniaxial yield stress, E is Young's modulus and H is a constant, typically in the order of 10^{-2}. The assumptions (1) and (2) are not necessarily suitable for accurate modeling of concrete but do not affect the ability to capture the most important failure in concrete, that is failure in tension. We assume an associative flow rule and a simple relation between the hardening parameter and the rate of the plastic flow

$$\begin{aligned} \dot{\boldsymbol{\epsilon}}^{pl} &= \dot{\lambda}\frac{\partial f}{\partial \boldsymbol{\sigma}} \\ \dot{\kappa} &= \dot{\lambda} & (3) \end{aligned}$$

where $\boldsymbol{\epsilon}^{pl}$ is the plastic strain tensor and the scalar λ is usually referred to as the *plastic multiplier*. The relation (3) does not accurately represent hardening mechanisms in metals. Nevertheless, it is accurate enough for the purpose of the current study, since post-yielding response of the steel phase should not have an effect on the optimal choice of material.

Throughout this study, we follow the framework described by Michaleris et al. [16] for nonlinear finite element analysis and adjoint sensitivity analysis, where the elasto-plastic nonlinear analysis is seen as a transient, nonlinear coupled problem. In the coupled approach, for every increment n in the transient analysis, we determine the unknowns $\mathbf{u}_n$ (displacements) and $\mathbf{v}_n$ (stresses and plastic multipliers) that satisfy the residual equations

$$\begin{aligned} \mathbf{R}_n(\mathbf{u}_n, \mathbf{u}_{n-1}, \mathbf{v}_n, \mathbf{v}_{n-1}) &= 0 & (4) \\ \mathbf{H}_n(\mathbf{u}_n, \mathbf{u}_{n-1}, \mathbf{v}_n, \mathbf{v}_{n-1}) &= 0 \end{aligned}$$

where $\mathbf{R}_n = 0$ is satisfied at the global level and $\mathbf{H}_n = 0$ is satisfied at each Gauss point. The transient, coupled and nonlinear system of equations is uncoupled by treating the response $\mathbf{v}$ as a function of the response $\mathbf{u}$. When solving the residual equations for the n-th "time" increment, the responses $\mathbf{u}_{n-1}$ and $\mathbf{v}_{n-1}$ are known from the previous converged increment. The independent response $\mathbf{u}_n$ is found by an iterative prediction-correction procedure in the global level, while for each iterative step the dependent

response $\mathbf{v}_n(\mathbf{u}_n)$ is found by an inner iterative loop. The responses $\mathbf{u}_n$ and its dependant $\mathbf{v}_n$ are corrected until Eq. (4) is satisfied to sufficient accuracy. This procedure is repeated for all N increments.

Neglecting body forces, $\mathbf{R}_n$ is defined as the difference between external and internal forces and depends explicitly only on $\mathbf{v}_n$

$$\mathbf{R}_n(\mathbf{v}_n) = \mathbf{f}_n - \int_V \mathbf{B}^T \boldsymbol{\sigma}_n dV$$

where $\mathbf{B}$ is the standard strain-displacement matrix in the context of finite element procedures. The internal, Gauss-point level variables $\mathbf{v}_n$ are defined as

$$\mathbf{v}_n = \left[\begin{array}{c} \boldsymbol{\sigma}_n \\ \lambda_n \end{array} \right]$$

where $\boldsymbol{\sigma}_n$ are the stresses and λ_n is the plastic multiplier. Furthermore, the residual $\mathbf{H}_n$ is defined as the collection of two incremental residuals

$$\mathbf{H}_n(\mathbf{u}_n, \mathbf{u}_{n-1}, \mathbf{v}_n, \mathbf{v}_{n-1}) = \left[\begin{array}{c} \mathbf{B}\mathbf{u}_n - \mathbf{B}\mathbf{u}_{n-1} - \mathbf{D}^{-1}(\boldsymbol{\sigma}_n - \boldsymbol{\sigma}_{n-1}) - \frac{\partial f}{\partial \boldsymbol{\sigma}_n}(\lambda_n - \lambda_{n-1}) \\ \sqrt{3J_2} + \alpha I_1 - \sigma_y(\lambda_n) \end{array} \right] = \mathbf{0} \qquad (5)$$

Here, the first equation equates total, elastic and plastic strains and the second represents the requirement that during plastic response the stress state satisfies the yield condition. In case an elastic step is predicted by the trial state, then no plastic flow occurs and $\lambda_n = \lambda_{n-1}$. Therefore the first equation is satisfied trivially by the elastic stress-strain relationship and the second equation can be disregarded.

The elasto-plastic problem is path-dependent by nature, meaning that the evolution of plastic strains under a certain load intensity depends on the history of plastic straining and cannot be computed correctly in one load stage. In practice, this means that the FE analysis must be solved incrementally. The default choice for most nonlinear FE solvers is to use *load control*, meaning that the total load is divided into a certain number of increments. Then for each increment, the current stress and strain states are required for the solution of the local elasto-plastic problem corresponding to the next load step. In some cases it is beneficial to switch to *displacement control*, for example when a small addition to the load causes a large additional displacement or when limit points are encountered [8]. In the context of optimal design, a fixed load intensity throughout the optimization process may cause difficulties in solving the nonlinear analysis equations for intermediate designs that are very flexible. From this point of view, using displacement control for the nonlinear analysis is preferable. This means that the displacement at a selected degree of freedom is prescribed to a certain value for all design cycles. Choosing an appropriate value is possible if the designer has some knowledge regarding the expected deformation, and can also be seen as a way of imposing a required deflection at a certain point. Displacement control was utilized also in previous studies regarding topology optimization of elasto-plastic structures, e.g. by Swan and Kosaka [21] and Maute et al. [15].

For these reasons we mainly use displacement control and corresponding objective functions in this study. Then the global residual equation (4) takes the form

$$\mathbf{R}_n(\mathbf{v}_n, \theta_n) = \theta_n \hat{\mathbf{f}} - \int_V \mathbf{B}^T \boldsymbol{\sigma}_n dV$$

where θ_n is the (unknown) load factor in the n-th increment and $\hat{\mathbf{f}}$ is a constant reference load vector with non-zero entries only at loaded degrees of freedom. When solving the coupled equation system for each increment, a single displacement has a prescribed value and the rest, as well as the corresponding load factor θ_n, are determined from equilibrium.

6. Problem formulation

For the purpose of optimizing the layout of reinforced concrete structures, we follow the material distribution approach for topological design [2] together with the SIMP (Solid Isotropic Material with Penalization) interpolation scheme [13]. The main idea is to interpolate the nonlinear behavior of the two candidate materials using the density variables from the topology optimization problem. The interpolation of the elastic modulus is identical to that used in standard, linear elastic topology optimization

$$E(\rho_e) = E_{min} + (E_{max} - E_{min})\rho_e^{p_E} \qquad (6)$$

where ρ_e is the density design variable corresponding to a certain finite element e. Interpolation of the nonlinear response is achieved by adding a dependency on the design variable ρ to the yield function

$$f(\boldsymbol{\sigma}, \lambda, \rho_e) = \sqrt{3J_2} + \alpha(\rho_e)I_1 - \sigma_y(\lambda, \rho_e) \tag{7}$$

Following a SIMP-type approach, the interpolating functions $\alpha(\rho_e)$ and $\sigma_y(\rho_e)$ are given by

$$\alpha(\rho_e) = \alpha_{max} - (\alpha_{max} - \alpha_{min})\rho_e^{p_\alpha} \tag{8}$$
$$\sigma_y(\lambda, \rho_e) = \sigma_{y,min}^0 + (\sigma_{y,max}^0 - \sigma_{y,min}^0)\rho_e^{p_{\sigma_y}} + HE(\rho_e)\lambda \tag{9}$$

where p_α and p_{σ_y} are penalization factors for α and σ_y, respectively. These interpolations imply that the yield surface of one material is obtained by choosing $\rho_e = 0$, meaning $\alpha = \alpha_{max}$ and $\sigma_y^0 = \sigma_{y,min}^0$, and the second yield surface is obtained by $\rho_e = 1$, meaning $\alpha = \alpha_{min}$ and $\sigma_y^0 = \sigma_{y,max}^0$. As stated above, the particular case $\alpha_{min} = 0$ means that the plastic response of the second material is governed by the von Mises yield criterion. By setting also $\sigma_{y,max}^0 = \sigma_{y,steel}^0$ an actual model of steel is obtained for $\rho_e = 1$. In Figure 1, the interpolation of the yield surfaces is demonstrated, for two materials resembling steel and concrete.
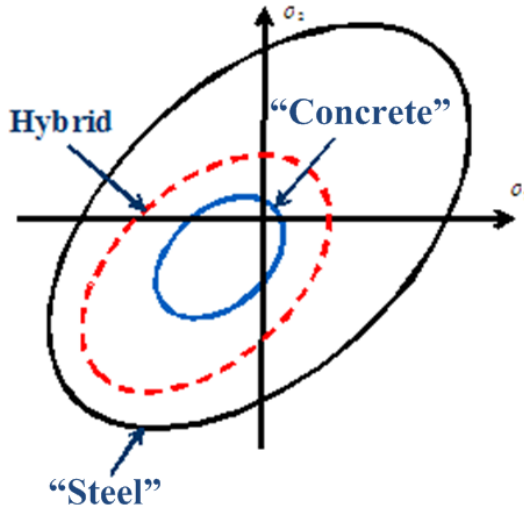

Figure 1: Demonstrative example of the interpolation between two yield surfaces, presented in 2D principal stress space. The "Hybrid" surface represents the behavior of an artificial mixture, corresponding to an intermediate density in topology optimization.

In order to approach optimal strut-and-tie designs, we extend this interpolation so it accommodates also void regions. Following [3], we add another design variable x for each finite element. Void regions are represented by $x = 0$ and solid regions are represented by $x = 1$. Within the solid regions, the value of ρ determines the distribution of the two candidate materials. This leads to the following interpolation functions, replacing Eqs. (6), (7), (8), (9)

$$E(x_e, \rho_e) = x_e^{p_{Ex}}(E_{min} + (E_{max} - E_{min})\rho_e^{p_E}) \tag{10}$$
$$f(\boldsymbol{\sigma}, \lambda, \rho_e, x_e) = \sqrt{3J_2} + \alpha(x_e, \rho_e)I_1 - \sigma_y(\lambda, x_e, \rho_e) = 0 \tag{11}$$
$$\alpha(x_e, \rho_e) = x_e^{p_{\alpha x}}(\alpha_{max} - (\alpha_{max} - \alpha_{min})\rho_e^{p_\alpha}) \tag{12}$$
$$\sigma_y(\lambda, x_e, \rho_e) = x_e^{p_{\sigma x}}(\sigma_{y,min}^0 + (\sigma_{y,max}^0 - \sigma_{y,min}^0)\rho_e^{p_{\sigma_y}} + HE(x_e, \rho_e)\lambda) \tag{13}$$

where p_{Ex}, $p_{\alpha x}$ and $p_{\sigma x}$ are penalization factors for x. In practice, one may choose to use the same penalty factors for both design variables, x and ρ.

In this article, we focus mainly on one demonstrative class of objective functions. The aim is to find the stiffest structural layouts given certain amounts of available material. When only linear elastic response is considered, the corresponding objective is the widely used minimum compliance problem. When nonlinear response is taken into account, one may define several different objectives that are related to the maximization of the structural stiffness (see for example [21], [15], [7]). Since displacement

control is preferred in the nonlinear FE analysis, a possible equivalent to minimizing compliance in linear elasticity is maximizing the end compliance for a given prescribed displacement. In other words, the objective is to maximize the magnitude of the load that corresponds to a certain prescribed displacement at a particular degree of freedom.

Assuming the analysis problem is solved in N increments, the optimization problem of distributing two materials and void in the design domain can be stated as follows

$$\min_{\boldsymbol{\rho},\mathbf{x}} c(\boldsymbol{\rho},\mathbf{x}) \quad = \quad -\theta_N \hat{\mathbf{f}}^T \mathbf{u}_N$$

$$\text{s.t.:} \quad \sum_{e=1}^{N_e} v_e x_e \leq V_1$$

$$\sum_{e=1}^{N_e} v_e \rho_e \leq V_2$$

$$0 < x_{min} \leq x_e \leq 1, \qquad e = 1, ..., N_e$$

$$0 \leq \rho_e \leq 1, \qquad e = 1, ..., N_e$$

$$\text{with the coupled residuals:} \quad \mathbf{R}_n(\mathbf{v}_n, \theta_n) = 0 \qquad n = 1, ..., N$$

$$\mathbf{H}_n(\mathbf{u}_n, \mathbf{u}_{n-1}, \mathbf{v}_n, \mathbf{v}_{n-1}, \boldsymbol{\rho}, \mathbf{x}) = 0 \qquad n = 1, ..., N \qquad (14)$$

where V_1 is the total available volume of material, V_2 is the available volume of the material whose properties correspond to $\rho_e = 1$ ($V_2 \leq V_1$) and x_{min} is a positive lower bound used in order to avoid singularity of the stiffness matrix. The problem of distributing two materials with no voids can be seen as a particular case of this formulation.

As mentioned earlier, the design sensitivities are computed by the adjoint method, following the framework for transient, nonlinear coupled problems described by Michaleris et al. [16]. To the best of the authors' knowledge, this is the first implementation of this framework in topology optimization of structures with material nonlinearities. Furthermore, it is presumably the first sensitivity analysis for topology optimization of structures with material nonlinearities where no simplifying assumptions are made. An effort is made to use similar notation to that in [16]. The procedure for sensitivity analysis is described here only for the two material and void problem (14) since the two-material problem can easily be deduced from it. We begin by forming the augmented objective function $\hat{c}(\boldsymbol{\rho})$

$$\hat{c}(\boldsymbol{\rho},\mathbf{x}) \quad = \quad -\theta_N \hat{\mathbf{f}}^T \mathbf{u}_N - \sum_{n=1}^{N} \boldsymbol{\lambda}_n^T \mathbf{R}_n(\mathbf{v}_n, \theta_n)$$

$$- \sum_{n=1}^{N} \boldsymbol{\gamma}_n^T \mathbf{H}_n(\mathbf{u}_n, \mathbf{u}_{n-1}, \mathbf{v}_n, \mathbf{v}_{n-1}, \boldsymbol{\rho}, \mathbf{x})$$

where $\boldsymbol{\lambda}_n$ and $\boldsymbol{\gamma}_n$ are the adjoint vectors to be found for all increments $n = 1, ..., N$. We assume the initial responses $\mathbf{u}_0$, $\mathbf{v}_0$ do not depend on the design variables. Furthermore, it can be observed that the objective function and the nonlinear equation systems $\mathbf{R}_n = 0$ ($n = 1, ..., N$) do not depend explicitly on the design variables. Therefore the explicit terms in the derivative of the augmented objective with respect to the design variables are

$$\frac{\partial \hat{c}_{exp}}{\partial x_e} \quad = \quad -\sum_{n=1}^{N} \boldsymbol{\gamma}_n^T \frac{\partial \mathbf{H}_n}{\partial x_e}$$

$$\frac{\partial \hat{c}_{exp}}{\partial \rho_e} \quad = \quad -\sum_{n=1}^{N} \boldsymbol{\gamma}_n^T \frac{\partial \mathbf{H}_n}{\partial \rho_e}$$

The adjoint vectors $\boldsymbol{\gamma}_n$ ($n = 1, ..., N$) are computed on a Gauss-point level by a backward incremental procedure, which is required due to path dependency of the elasto-plastic response. The backward procedure consists of the collection of equation systems resulting from the requirement that all implicit derivatives of the design variables will vanish. Further details regarding the adjoint procedure can be found in [1]. For performing the backwards-incremental sensitivity analysis, the derivatives of the global and local residuals with respect to the analysis variables are required. These are given in this section for

the elasto-plastic model utilized in the current study. In particular, we consider a plane stress situation, meaning the stresses and strains are collected in a vector with three entries: $\boldsymbol{\sigma} = [\sigma_{11}, \sigma_{22}, \sigma_{12}]^T$ and $\boldsymbol{\epsilon} = [\epsilon_{11}, \epsilon_{22}, \epsilon_{12}]^T$.

The derivative of the global residual is independent of the specific material model employed and is given by

$$\frac{\partial(\mathbf{R}_n)}{\partial(\mathbf{v}_n)} = \begin{bmatrix} -\mathbf{B}^T w J_{(8\times3)} & \mathbf{0}_{(8\times1)} \end{bmatrix}$$

where $\mathbf{B}$ is the standard strain-displacement matrix; w is the Gauss-point weight for numerical integration; and J is the determinant of the Jacobian at the Gauss-point. For the nonlinear material model described in Section 5, the derivatives of the local residual are

$$\frac{\partial(\mathbf{H}_n)}{\partial(\mathbf{u}_n)} = \begin{bmatrix} \mathbf{B}_{(3\times8)} \\ \mathbf{0}_{(1\times8)} \end{bmatrix}$$

$$\frac{\partial(\mathbf{H}_{n+1})}{\partial(\mathbf{u}_n)} = \begin{bmatrix} -\mathbf{B}_{(3\times8)} \\ \mathbf{0}_{(1\times8)} \end{bmatrix}$$

$$\frac{\partial(\mathbf{H}_n)}{\partial(\mathbf{v}_n)} = \begin{bmatrix} -\mathbf{D}^{-1} - \Delta^n \lambda \frac{\partial^2 f}{\partial \boldsymbol{\sigma}_n}{}_{(3\times3)} & -\frac{\partial f}{\partial \boldsymbol{\sigma}_n}^T{}_{(3\times1)} \\ \frac{\partial f}{\partial \boldsymbol{\sigma}_n}{}_{(1\times3)} & -HE_{(1\times1)} \end{bmatrix}$$

$$\frac{\partial(\mathbf{H}_{n+1})}{\partial(\mathbf{v}_n)} = \begin{bmatrix} \mathbf{D}^{-1}{}_{(3\times3)} & \frac{\partial f}{\partial \boldsymbol{\sigma}_{n+1}}^T{}_{(3\times1)} \\ \mathbf{0}_{(1\times3)} & 0_{(1\times1)} \end{bmatrix}$$

where the derivative of the yield function with respect to the stress components is

$$\frac{\partial f}{\partial \boldsymbol{\sigma}} = \frac{1}{2\sqrt{3J_2}} \begin{bmatrix} 2\sigma_{11} - \sigma_{22} & 2\sigma_{22} - \sigma11 & 6\sigma_{12} \end{bmatrix} + \alpha \begin{bmatrix} 1 & 1 & 0 \end{bmatrix}$$

In actual implementation, the derivatives of the local residuals $\mathbf{H}_n$ and $\mathbf{H}_{n+1}$ should maintain consistency with respect to the analysis. This means that some rows and columns should be disregarded in case of elastic loading or unloading. For example, if increment n is elastic, then we have $\frac{\partial(\mathbf{H}_n)}{\partial(\mathbf{u}_n)} = \begin{bmatrix} \mathbf{B}_{(3\times8)} \end{bmatrix}$ and $\frac{\partial(\mathbf{H}_n)}{\partial(\mathbf{v}_n)} = \begin{bmatrix} -\mathbf{D}^{-1}_{(3\times3)} \end{bmatrix}$.

Finally, computing the derivatives $\frac{\partial \mathbf{H}_n}{\partial x_e}$, $\frac{\partial \mathbf{H}_n}{\partial \rho_e}$ requires adding the dependency on the design variables to Eq. (5) and differentiating with respect to x_e and ρ_e. This leads to

$$\frac{\partial \mathbf{H}_n}{\partial x_e} = \begin{bmatrix} -\frac{\partial(\mathbf{D}(x_e,\rho_e)^{-1})}{\partial x_e}(\boldsymbol{\sigma}_n - \boldsymbol{\sigma}_{n-1}) - \frac{\partial(\frac{\partial f}{\partial \boldsymbol{\sigma}_n}(x_e,\rho_e))^T}{\partial x_e}(\lambda_n - \lambda_{n-1}) \\ \frac{\partial f(x_e,\rho_e)}{\partial x_e} \end{bmatrix}$$

$$\frac{\partial \mathbf{H}_n}{\partial \rho_e} = \begin{bmatrix} -\frac{\partial(\mathbf{D}(x_e,\rho_e)^{-1})}{\partial \rho_e}(\boldsymbol{\sigma}_n - \boldsymbol{\sigma}_{n-1}) - \frac{\partial(\frac{\partial f}{\partial \boldsymbol{\sigma}_n}(x_e,\rho_e))^T}{\partial \rho_e}(\lambda_n - \lambda_{n-1}) \\ \frac{\partial f(x_e,\rho_e)}{\partial \rho_e} \end{bmatrix}$$

where

$$\frac{\partial(\mathbf{D}(x_e,\rho_e)^{-1})}{\partial x_e} = -\frac{1}{E(x_e,\rho_e)}\frac{\partial E(x_e,\rho_e)}{\partial x_e}\mathbf{D}(x_e,\rho_e)^{-1}$$

$$\frac{\partial(\mathbf{D}(x_e,\rho_e)^{-1})}{\partial \rho_e} = -\frac{1}{E(x_e,\rho_e)}\frac{\partial E(x_e,\rho_e)}{\partial \rho_e}\mathbf{D}(x_e,\rho_e)^{-1}$$

$$\frac{\partial(\frac{\partial f}{\partial \boldsymbol{\sigma}_n}(x_e,\rho_e))^T}{\partial x_e} = \frac{\partial \alpha(x_e,\rho_e)}{\partial x_e}\begin{bmatrix} 1 \\ 1 \\ 0 \end{bmatrix}$$

$$\frac{\partial(\frac{\partial f}{\partial \boldsymbol{\sigma}_n}(x_e,\rho_e))^T}{\partial \rho_e} = \frac{\partial \alpha(x_e,\rho_e)}{\partial \rho_e}\begin{bmatrix} 1 \\ 1 \\ 0 \end{bmatrix}$$

$$\frac{\partial f(x_e,\rho_e)}{\partial x_e} = \frac{\partial \alpha(x_e,\rho_e)}{\partial x_e}I_1 - \frac{\partial \sigma_y(x_e,\rho_e)}{\partial x_e}$$

$$\frac{\partial f(x_e,\rho_e)}{\partial \rho_e} = \frac{\partial \alpha(x_e,\rho_e)}{\partial \rho_e}I_1 - \frac{\partial \sigma_y(x_e,\rho_e)}{\partial \rho_e}$$

The above derivatives can be easily computed using the relations given in Eqs. (10), (11), (12), (13).

Remarks regarding sensitivity analysis for displacement-controlled analysis The objective function used in the problem formulations above is appropriate for stiffness maximization only in the case of a single point load. Applying a distributed load while prescribing a single displacement poses a problem when defining a proper objective for stiffness maximization. As discussed in [1], maximizing the global end-compliance $\theta \widehat{\mathbf{f}}_{ext}^T \mathbf{u}$ may result in a structure that is very stiff with respect to bearing the load at the prescribed DOF but very flexible with respect to all other loads. Therefore when a distributed load is applied, the objective is defined as minimizing the end-compliance $\mathbf{f}_{ext}^T \mathbf{u}$ *as if* the analysis is load-controlled and *as if* the load intensity is constant throughout the optimization. The resulting hybrid procedure combines the advantages of both load and displacement control. On the one hand, the analysis is more stable numerically and is more likely to converge when the structural layout is relatively "soft". On the other hand, the objective is well-defined and should lead to the best global stiffness with respect to all the applied loads. In practice, this can be seen as a load-controlled procedure, just that the load intensity varies throughout the design process to fit the prescribed displacement. Moreover, in the sensitivity analysis it is assumed that the solution was obtained using load control, which leads to a more straightforward computational procedure. Further details can be found in [1].

7. Examples

In this section we present several results obtained when implementing the computational approach described in this article. The purpose is to demonstrate the capabilities and potential of our approach and to gain insight regarding implementation aspects. Therefore, as preliminary examples we consider relatively small scale two-dimensional problems with no self weight. Extending to three dimensional models and incorporating more realistic loading conditions are among the goals of future work.

The examples presented refer to both the distribution of concrete and steel as well as to the distribution of concrete, steel and void (14). The material parameters resemble actual values corresponding to steel and concrete, see Table 1. For computing α_{max} and $\sigma_{y,min}^0$, both corresponding to the concrete phase, it was assumed that the strength of concrete in compression is ten times higher than in tension. All test cases were solved using a 2D finite element mesh consisting of square, bi-linear plane stress elements. The optimization was performed by a nonlinear optimization program based on the Method of Moving Asymptotes - MMA [20]. In order to obtain regularized designs and to avoid checkerboard patterns, a density filter was applied [4, 6].

Table 1: Material properties in all test cases

Parameter	Material	Value
E_{min}	concrete	25.0 [GPa]
E_{max}	steel	200.0 [GPa]
α_{min}	steel	0.0
α_{max}	concrete	0.818
$\sigma_{y,min}^0$	concrete	5.5 [MPa]
$\sigma_{y,max}^0$	steel	300 [MPa]
ν	both	0.3
H	both	0.01

7.1. Optimized beams subject to distributed loads

In these example problems, we again address the maximum end-compliance design of beams. We consider more slender beams with loads evenly distributed along the length, see Figure 2(a) for the setup of a simply supported beam and Figure 3(a) for the setup of a cantilevered beam. Due to the larger length-to-height ratio, we expect bending action to be much more dominant than in the previous example. The models of the symmetric halves are discretized with 160×40 and 240×40 FE meshes respectively; the volume fraction is set to 0.1 for both cases; and the load is modeled as 10 equally spaced point loads on one half of the beam. For the simply supported beam, we apply a prescribed displacement directed downwards at the mid point of the top fiber, with a magnitude of $\delta = 0.005$. For the cantilevered beam, the prescribed displacement is at the top of the free edge and the magnitude is $\delta = 0.001$.

Examining the layouts obtained with distributed loads, it can be seen that the presented procedure enables a clear distinction between tensile and compressive stresses. In the simply supported beam, steel reinforcement is placed in the bottom fiber where tensile stresses appear due to bending, and in the vicinity

of concentrated forces (at the supports in this case). Near the supports, the bottom fiber reinforcement is bent upwards. This improves the structure's resistance to shear failure, which is dominant in these regions. In the cantilevered beam, the same principals are followed, so steel is added also to the top fiber above the supports. This reinforcement is bent in both directions according to the varying dominance of shear failure in comparison to bending failure. Finally, it can be observed that small portions of steel are used also to reinforce the support regions and to a lesser extent under loading points.
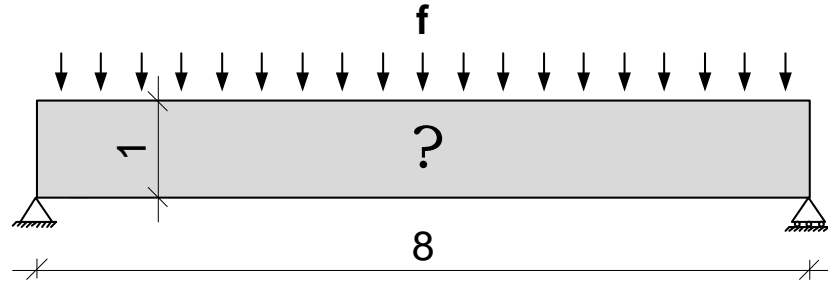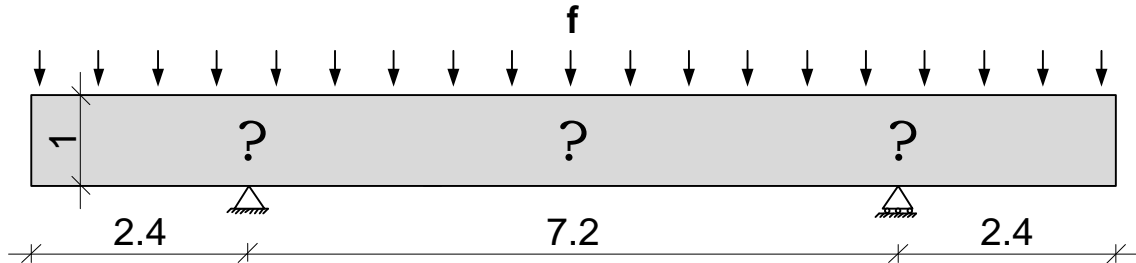

(a) Design domain and boundary conditions.

(b) Optimized layout after 150 design iterations with gradual refinement.

Figure 2: Maximum end-compliance of a simply supported beam subject to a distributed load. Black = steel, white = concrete. Steel consists of 10% of the total volume.

(a) Design domain and boundary conditions.

(b) Optimized layout after 300 design iterations with gradual refinement.

Figure 3: Maximum end-compliance of a cantilevered beam subject to a distributed load. Black = steel, white = concrete. Steel consists of 10% of the total volume.

7.2. Optimized short cantilever

In this example problem, the proposed procedure is applied for designing the reinforcement in a short cantilever. The design domain is a square supported at two corners on the left side and loaded with a prescribed displacement directed downwards at the opposite bottom corner. The model is discretized with a 100×100 FE mesh. The objective is to maximize the end-compliance, and we present two results: one of concrete-steel distribution and another of concrete-steel-void distribution. For the two-material design, the steel volume fraction is 0.2. When void is considered as well, then the total volume fraction is 0.4 and the steel volume fraction is 0.1. The prescribed displacements are set to $\delta = 0.002$ and $\delta = 0.001$

respectively. The penalty factors are set to the value of 3.0 and the filter radius is $r = 0.015$ for all design iterations.
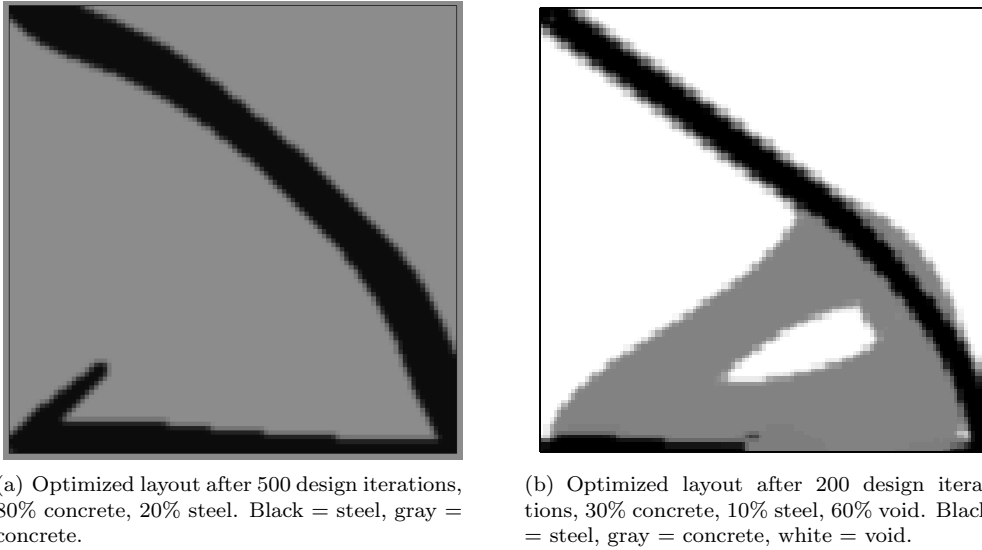

(a) Optimized layout after 500 design iterations, 80% concrete, 20% steel. Black = steel, gray = concrete.

(b) Optimized layout after 200 design iterations, 30% concrete, 10% steel, 60% void. Black = steel, gray = concrete, white = void.

Figure 4: Maximum end-compliance of a short cantilever

In both cases, steel is used mainly for a cable-like member in tension, transferring the load to the upper support. This cable is then supported by either a continuous concrete domain (when no voids are possible) or by two compressed concrete bars, see Figures 4(a), 4(b). This again demonstrates the capability of the procedure to distinguish between structural elements in tension and in compression and to choose the appropriate material for each type. The layout obtained when distributing steel, concrete and void resembles strut-and-tie models that are widely used in practical analysis and design of reinforced concrete. As observed in previous examples, steel might be used also for stiffening support regions. In the short cantilever, this is the case mainly for the two material problem with no voids. To a lesser extent, this is observed also in the result of the concrete-steel-void distribution.

8. Discussion

The resulting optimized layouts clearly demonstrate the potential of this approach. When distributing steel within a concrete beam, the placement of reinforcement resembles traditional design and agrees with common engineering knowledge. When distributing concrete, steel and void, it is shown that optimized strut-and-tie models are generated. These can be used for several purposes: first, to provide the engineer an improved initial design before the detailed design stage; second, to challenge traditional practice and achieve more efficient design of reinforced concrete structures by suggesting non-traditional forms and shapes; third, to reduce weight and concrete production, by utilizing lightweight concrete in the "void" regions where no strength is required.

Future work will focus on more realistic modeling. With respect to loading conditions, it is necessary to consider also self-weight and multiple load cases. Another important issue is the constraint on the volume of reinforcing material: in practice, the relative volume of steel seldom exceeds 1%. This requires much more refined FE models in which thin steel bars can be properly realized. Another important extension is to consider strain softening in the concrete phase. Consequently, transferring tension forces in concrete will be even less preferable, meaning that more realistic designs can be suggested. Finally, the introduction of other objective functions will also be explored.

9. Acknowledgments

10. References

[1] O. Amir. *Efficient Reanalysis Procedures in Structural Topology Optimization*. PhD thesis, Technical University of Denmark, 2011.

[2] M. P. Bendsøe and N. Kikuchi. Generating optimal topologies in structural design using a homogenization method. *Computer Methods in Applied Mechanics and Engineering*, 71:197–224, 1988.

[3] M. P. Bendsøe and O. Sigmund. *Topology Optimization - Theory, Methods and Applications*. Springer, Berlin, 2003.

[4] B. Bourdin. Filters in topology optimization. *International Journal for Numerical Methods in Engineering*, 50:2143–2158, 2001.

[5] M. Bruggi. Generating strut-and-tie patterns for reinforced concrete structures using topology optimization. *Computers and Structures*, 87(23-24):1483–1495, 2009.

[6] T. E. Bruns and D. A. Tortorelli. Topology optimization of non-linear elastic structures and compliant mechanisms. *Computer Methods in Applied Mechanics and Engineering*, 190:3443–3459, 2001.

[7] T. Buhl, C. Pedersen, and O. Sigmund. Stiffness design of geometrically nonlinear structures using topology optimization. *Structural and Multidisciplinary Optimization*, 19(2):93–104, 2000.

[8] M. A. Crisfield. *Non-linear Finite Element Analysis of Solids and Structures*, volume 1. John Wiley & Sons, 1991.

[9] D. C. Drucker and W. Prager. Soil mechanics and plastic analysis or limit design. *Quarterly of Applied Mathematics*, 10(2):157–165, 1952.

[10] J. Kato, A. Lipka, and E. Ramm. Multiphase material optimization for fiber reinforced composites with strain softening. *Structural and Multidisciplinary Optimization*, 39(1):63–81, 2009.

[11] H.-G. Kwak and S.-H. Noh. Determination of strut-and-tie models using evolutionary structural optimization. *Engineering Structures*, 28(10):1440–1449, 2006.

[12] Q. Liang, Y. Xie, and G. Steven. Topology optimization of strut-and-tie models in reinforced concrete structures using an evolutionary procedure. *ACI Structural Journal*, 97(2):322–330, 2000.

[13] M. P. Bendsøe. Optimal shape design as a material distribution problem. *Structural Optimization*, 1:193–202, 1989.

[14] P. Marti. Truss models in detailing. *Concrete International*, 7:66–73, 1985.

[15] K. Maute, S. Schwarz, and E. Ramm. Adaptive topology optimization of elastoplastic structures. *Structural Optimization*, 15(2):81–91, 1998.

[16] P. Michaleris, D. A. Tortorelli, and C. A. Vidal. Tangent operators and design sensitivity formulations for transient non-linear coupled problems with applications to elastoplasticity. *International Journal for Numerical Methods in Engineering*, 37:2471–2499, 1994.

[17] W. Ritter. The hennebique system of construction. *Schweizerische Bauzeitung*, 33/34, 1899.

[18] J. Schlaich, K. Schafer, and M. Jennewein. Toward a consistent design of structural concrete. *PCI Journal*, 32(3):74–150, 1987.

[19] J. Simo and T. Hughes. *Computational Inelasticity*. Springer, New York, 1998.

[20] K. Svanberg. The method of moving asymptotes - a new method for structural optimization. *International Journal for Numerical Methods in Engineering*, 24:359–373, 1987.

[21] C. Swan and I. Kosaka. Voigt-Reuss topology optimization for structures with nonlinear material behaviors. *International Journal for Numerical Methods in Engineering*, 40(20):3785–3814, 1997.

[22] O. C. Zienkiewicz and R. L. Taylor. *The Finite Element Method (5th edition) Volume 2 - Solid Mechanics*. Elsevier, 2000.